Vortex pinning in the superfluid core of neutron stars and the rise of pulsar glitches

Aurélien Sourie, Nicolas Chamel

Monthly Notices of the ROYAL ASTRONOMICAL SOCIETY

MNRAS **493,** L98–L102 (2020) doi:10.1093/mnrasl/slaa015
Advance Access publication 2020 January 28

Vortex pinning in the superfluid core of neutron stars and the rise of pulsar glitches

Aurélien Sourie[1,2]★ and Nicolas Chamel[1]★

[1]*Institut d'Astronomie et d'Astrophysique, Université Libre de Bruxelles, CP-226, B-1050 Brussels, Belgium*
[2]*Laboratoire Univers et Théories, Observatoire de Paris, Université PSL, CNRS, Université de Paris, F-92190 Meudon, France*

Accepted 2020 January 21. Received 2020 January 18; in original form 2019 December 12

ABSTRACT

Timing of the Crab and Vela pulsars has recently revealed very peculiar evolutions of their spin frequency during the early stage of a glitch. We show that these differences can be interpreted from the interactions between neutron superfluid vortices and proton fluxoids in the core of these neutron stars. In particular, pinning of individual vortices to fluxoids is found to have a dramatic impact on the mutual friction between the neutron superfluid and the rest of the star. The number of fluxoids attached to vortices turns out to be a key parameter governing the global dynamics of the star. These results may have implications for the interpretation of other astrophysical phenomena such as pulsar-free precession or the r-mode instability.

Key words: stars: neutron – pulsars: individual: (PSR B0833−45, PSR B0531+21).

1 INTRODUCTION

Pulsars are neutron stars (NSs) spinning very rapidly with extremely stable periods. With relative delays as small as 10^{-21}, some pulsars outperform the most accurate terrestrial clocks (Milner et al. 2019). Nevertheless, irregularities have been detected in long-term pulsar-timing observations. In particular, some pulsars have been found to suddenly spin up. Such 'glitches' in their rotational frequency Ω, ranging from $\Delta\Omega/\Omega \sim 10^{-9}$ to $\sim 10^{-5}$, are sometimes accompanied by an abrupt change of the spin-down rate from $|\Delta\dot{\Omega}/\dot{\Omega}| \sim 10^{-6}$ up to $\sim 10^{-2}$ (Manchester 2017). At the time of this writing, 554 glitches have been detected in 190 pulsars[1] (Espinoza et al. 2011). The very long post-glitch relaxation, lasting from days to years, reveals the presence of superfluid components in NSs (Chamel 2017). Glitches themselves are thought to be the manifestations of superfluidity (Haskell & Melatos 2015). These events are commonly interpreted as sudden transfers of angular momentum from a more rapidly rotating neutron superfluid to the rest of star due to the catastrophic unpinning of quantized vortices. However, large uncertainties remain concerning the dynamics of these vortices. In particular, protons in the outer core of an NS are generally thought to form a type-II superconductor such that the magnetic flux penetrates through fluxoids, each carrying a magnetic flux quantum $\phi_0 = hc/(2e) \simeq 2 \times 10^{-7}$ G cm^2, where h is Planck's constant, c the speed of light, and e the proton electric charge. The mean surface density of fluxoids, $\mathcal{N}_\mathrm{p} \simeq 5 \times 10^{18}\, B_{12}$ cm^{-2} where $B_{12} = B/10^{12}$ G is the stellar internal magnetic field, is huge compared to that of vortices, $\mathcal{N}_\mathrm{n} \simeq 6 \times 10^5/P_{10}$ cm^{-2} where $P_{10} = P/10$ ms is the observed rotation period. Vortices may pin to fluxoids, and this may affect significantly the dynamical evolution of the star (Alpar 2017). Nevertheless, the role of the core superfluid on the glitch rise remains to be investigated.

So far, the most detailed information comes from the large glitches recently detected in the Vela (Palfreyman et al. 2018; Ashton et al. 2019) and Crab pulsars (Shaw et al. 2018), revealing very different behaviours. The analysis of the Vela glitch observed in 2016 December suggests the presence of an overshoot of amplitude[2] $\Delta f_\mathrm{over} \sim 19$–$38$ μHz, significantly larger than the amplitude of the pulsar frequency jump at the end of the rise stage, $\Delta f \simeq 16$ μHz. While the time-scale τ_r associated with the glitch rise is found to be shorter than ~ 12 s, a longer time-scale has been deduced for the subsequent decrease, $\tau_\mathrm{d} \sim 41$–125 s. These two time-scales are compatible with observations of previous Vela glitches (Dodson, McCulloch & Lewis 2002; Dodson, Lewis & McCulloch 2007). Furthermore, some evidence for the existence of a precursor (in the form of a rapid slow-down preceding the glitch) may have been found in the 2016 Vela glitch. On the other hand, a delayed spin-up, consisting of a first unresolved frequency jump Δf_short over a short time-scale τ_short followed by a resolved spin-up with an amplitude Δf_long over a longer time-scale τ_long, has been detected in the 1989, 1996, and 2017 Crab glitches (Lyne, Smith & Pritchard 1992; Wong, Backer & Lyne 2001; Shaw et al. 2018). The analysis of the 2017 Crab glitch has led to $\Delta f_\mathrm{short} \simeq 14$ μHz, $\Delta f_\mathrm{long} \simeq 1.1$ μHz, $\tau_\mathrm{short} \leq$

★ E-mail: aurelien.sourie@obspm.fr, asourie@ulb.ac.be (AS), nchamel@ulb.ac.be (NC)

[1]http://www.jb.man.ac.uk/pulsar/glitches/gTable.html

[2]The amplitude Δf_over given here corresponds to the magnitude of the exponentially decaying term plus that of the final frequency jump, denoted by Δf_d and Δf, respectively, in Ashton et al. (2019).

0.45 d, and $\tau_{\rm long} \simeq 1.7$ d, corresponding to a total amplitude $\Delta f = \Delta f_{\rm short} + \Delta f_{\rm long} \simeq 15$ μHz, and a total rise time $\tau_{\rm r} \sim \tau_{\rm short} + \tau_{\rm long} \sim 2$ d. Similar time-scales have been deduced from the analyses of the 1989 and 1996 glitches, but amplitudes ∼10 times smaller were observed. Finally, let us stress that the spin-up stage has not been resolved for smaller Crab glitches.

The glitch rise is thought to be governed by mutual-friction forces between the superfluid and the rest of the star, arising from the dissipative forces acting on individual vortices (Haskell & Melatos 2015; Sourie et al. 2017; Graber, Cumming & Andersson 2018; Haskell et al. 2018). Recently, Haskell et al. (2018) have suggested that the different spin-up evolutions observed in the Vela and Crab pulsars could be explained by the different stellar regions (core versus crust) where the glitch is driven. In this letter, we explore the impact of vortex pinning only in the outer core of NSs on the glitch rise.

2 SMOOTH-AVERAGED HYDRODYNAMIC DESCRIPTION

2.1 Forces on a single vortex

Let us consider a single neutron vortex pinned to $N_{\rm p}$ proton fluxoids and moving with velocity $v_{\rm L}^i$ ($i = 1, 2, 3$ denoting spatial indices). The vortex is assumed to be evolving in a mixture of superconducting protons, (degenerate) electrons, and superfluid neutrons at zero temperature. Although the arrangement of fluxoids in the core of an NS may be quite complicated, depending not only on the cooling and magnetorotational evolution of the star (Srinivasan et al. 1990; Ruderman, Zhu & Chen 1998; Jahan-Miri 2000) but also on the nature of the phase transition (Haber & Schmitt 2017), we suppose for simplicity that the $N_{\rm p}$ pinned fluxoids are aligned with the vortex (Ding, Cheng & Chau 1993; Ruderman et al. 1998). This assumption is actually not completely unrealistic, at least at small enough scales (Drummond & Melatos 2017). Note that the pinned fluxoids are not necessarily superimposed on the vortex. Vortex-fluxoid clusters may actually form naturally (Sedrakian & Sedrakian 1995). Here, $N_{\rm p}$ is an unknown parameter that could potentially be as large as $N_{\rm p}^{\rm max} \sim \mathcal{N}_{\rm p}/\mathcal{N}_{\rm n} \simeq 10^{13}\, B_{12}\, P_{10}$. We further assume that the vortex is straight, infinitely rigid and we ignore the effects of gravity giving rise to a buoyancy force (see Dommes & Gusakov 2017 for a recent discussion).

We determine the force felt by a single vortex moving in an asymptotically uniform superfluid mixture following an approach originally developed by Carter, Langlois & Prix (2002) in the relativistic framework, and later adapted to the Newtonian context by Carter & Chamel (2005). Making use of the results obtained by Gusakov (2019) for electrons, the force acting on the vortex can be decomposed into three parts: $\mathcal{F}^i = \mathcal{F}^i_{\rm Mn} + \mathcal{F}^i_{\rm Mp} + \mathcal{F}^i_{\rm d}$, as shown in an accompanying paper (Sourie & Chamel 2020). The neutron Magnus force arising from the relative flow of superfluid neutrons with velocity $v_{\rm n}^i - v_{\rm L}^i$ is given by

$$\mathcal{F}^i_{\rm Mn} = -\rho_{\rm n}\, \varepsilon^{ijk}\, \kappa\, \hat{\kappa}_j\, (v_{{\rm n}k} - v_{{\rm L}k})\,, \tag{1}$$

where $\rho_{\rm n}$ is the neutron mass density, $\kappa = h/(2\,m)$ is the quantum of circulation (m denoting the neutron rest mass, taken to be equal to that of protons), and $\hat{\kappa}^i$ is a unit vector oriented along the vortex. Likewise, the flow of protons with velocity $v_{\rm p}^i - v_{\rm L}^i$ relative to pinned fluxoids leads to a Magnus type force

$$\mathcal{F}^i_{\rm Mp} = -\rho_{\rm p}\, N_{\rm p}\, \varepsilon^{ijk}\, \kappa\, \hat{\kappa}_j\, \left(v_{{\rm p}k} - v_{{\rm L}k}\right), \tag{2}$$

where $\rho_{\rm p}$ is the proton mass density. The scattering of electrons off the magnetic field carried by fluxoids, and to a lesser extent that induced by entrained protons around the vortex (Alpar, Langer & Sauls 1984), leads to the drag force

$$\mathcal{F}^i_{\rm d} = -\rho_{\rm n}\, \kappa\, \xi\, \left(v_{\rm L}^i - v_{\rm p}^i\right), \tag{3}$$

where $\xi > 0$ is the so-called drag-to-lift ratio.

2.2 Global averaging over many vortices

On length-scales much larger than the intervortex separation, the electrically charged particles inside NSs are strongly coupled and essentially corotate with the crust and the magnetosphere (Glampedakis, Andersson & Samuelsson 2011). The outer core of an NS can therefore be reasonably well described by means of a two-fluid model, involving (i) a neutron superfluid moving with velocity $v_{\rm n}^i$ and (ii) a (viscous) charge-neutral fluid made of protons and electrons (simply labelled by 'p' in the following), moving with velocity $v_{\rm p}^i$. The two fluids are mutually coupled by friction forces induced by the drag force (3). The smooth-averaged force per unit volume exerted by the vortices on the superfluid (ignoring interactions between vortices) is given by

$$f^i_{\rm mf} = -\mathcal{N}_{\rm n}\, \mathcal{F}^i_{\rm Mn}\,. \tag{4}$$

Solving the force balance equation of a single vortex (neglecting its mass) $\mathcal{F}^i_{\rm d} + \mathcal{F}^i_{\rm Mn} + \mathcal{F}^i_{\rm Mp} = 0$ for the vortex velocity $v_{\rm L}^i$ following standard procedure (Hall & Vinen 1956) and substituting into (4) yields

$$f^i_{\rm mf} = -\mathcal{N}_{\rm n}\, \rho_{\rm n}\, \kappa\, \left(\mathcal{B}'\, \varepsilon^{ijk} \hat{\kappa}_j w^{\rm pn}_k + \mathcal{B}\, \varepsilon^{ijk} \hat{\kappa}_j \varepsilon_{klm} \hat{\kappa}^l w^m_{\rm pn}\right), \tag{5}$$

where $w^i_{\rm pn} = v^i_{\rm p} - v^i_{\rm n}$,

$$\mathcal{B} = \frac{\xi}{(1+X)^2 + \xi^2}\,,\ \mathcal{B}' = 1 - \frac{1+X}{(1+X)^2+\xi^2}\,,\ X = \frac{x_{\rm p}}{1-x_{\rm p}} N_{\rm p}, \tag{6}$$

$x_{\rm p} = \rho_{\rm p}/(\rho_{\rm p} + \rho_{\rm n})$ denoting the proton fraction. While expression (5) is formally similar to that obtained in the absence of pinning (Mendell 1991), pinning is found to affect the actual values of the mutual-friction coefficients (6) by (i) modifying the drag-to-lift ratio ξ, and (ii) inducing an extra dependence on X due to the proton Magnus force (2). The drag force remains poorly known. If the $N_{\rm p}$ fluxoids and the vortex are superimposed, $\xi \propto N_{\rm p}^2$ (Ding et al. 1993), while $\xi \propto N_{\rm p}$ according to the vortex-cluster model of Sedrakian & Sedrakian (1995). Given the current lack of knowledge, we adopt the following parametrization:[3]

$$\xi = \xi_0 \times \left(\varepsilon_{\rm p}\right)^{-2} \times \left(N_{\rm p}\right)^{\alpha} \quad \text{if } N_{\rm p} > 0\,, \tag{7}$$

where ξ_0 is the drag-to-lift ratio in the absence of pinning (Alpar et al. 1984; Mendell 1991; Andersson, Sidery & Comer 2006)

$$\xi_0 = 4 \times 10^{-4} \frac{\varepsilon_{\rm p}^2}{\left(1-\varepsilon_{\rm p}\right)^{1/2}} \left(\frac{x_{\rm p}}{0.05}\right)^{7/6} \frac{1}{1-x_{\rm p}} \rho_{14}{}^{1/6}\,, \tag{8}$$

$\varepsilon_{\rm p}$ denoting the proton entrainment parameter, and $\rho_{14} = \rho/(10^{14}\ {\rm g\ cm^{-3}})$ the mass density.

The mutual-friction coefficients are plotted in Fig. 1. The following typical values for the other parameters were adopted: $\varepsilon_{\rm p} =$

[3]The factor of $1/\varepsilon_{\rm p}^2$ is needed so as to recover known results for a single fluxoid (Gusakov 2019).

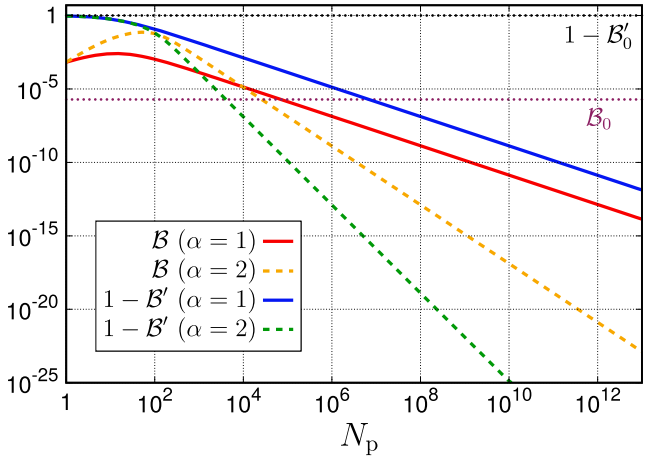

Figure 1. Mutual-friction coefficients $\mathcal{B}$ and $1-\mathcal{B}'$ in the outer core of NSs as functions of the number $N_{\rm p}$ of pinned fluxoids for $\alpha=1$ (solid lines) and $\alpha=2$ (dashed lines). Corresponding values for $N_{\rm p}=0$ are indicated as horizontal lines.

0.05, $x_{\rm p}=0.07$, and $\rho_{14}=2.7$. The mutual-friction coefficients $\mathcal{B}_0\equiv\mathcal{B}\left(N_{\rm p}=0\right)$ and $\mathcal{B}'_0\equiv\mathcal{B}'\left(N_{\rm p}=0\right)$ in the absence of pinning are displayed by horizontal lines in Fig. 1. For both values of α, $\mathcal{B}\gg\mathcal{B}_0$ for small enough values of $N_{\rm p}$, while the opposite behaviour is observed at higher $N_{\rm p}$. Moreover, $\mathcal{B}'\simeq\mathcal{B}'_0\simeq 0$ for $N_{\rm p}\gtrsim 0$, while $\mathcal{B}'\simeq 1$ at higher $N_{\rm p}$. Pinning may thus have a dramatic impact on the mutual-friction force and on the superfluid dynamics of NSs depending on $N_{\rm p}$. Similar conclusions can be drawn for any real value of α.

3 ASTROPHYSICAL IMPLICATIONS FOR PULSAR GLITCHES

3.1 Minimal model

To investigate the impact of core vortex pinning on the glitch dynamics, we consider a 'minimal' model in which the NS is simply described in terms of three dynamically distinct components: (i) a 'pinned' neutron superfluid in the outer core where the magnetic field is predominantly toroidal and pinning to fluxoids is expected to be the most effective (Haskell, Pizzochero & Seveso 2013; Gügercinoğlu & Alpar 2014), (ii) a 'non-pinned' neutron superfluid in the inner core, and (iii) the rest of the star. In view of the strong entrainment in the crust (Chamel 2012), we assume for simplicity that only the core neutron superfluid participates to the glitch. The third component, simply referred to as 'proton' in the following, thus consists of all charged particles (protons, leptons, nuclei in the crust) and the crustal neutron superfluid. All three components are rigidly rotating around a common axis, z say, at the angular velocity $\Omega_{\rm n}^{\rm pin}$, $\Omega_{\rm n}^{\rm f}$, and $\Omega_{\rm p}$, respectively. The corresponding moments of inertia are denoted by $I_{\rm n}^{\rm pin}$, $I_{\rm n}^{\rm f}$, and $I_{\rm p}$, and satisfy $I_{\rm n}^{\rm pin}+I_{\rm n}^{\rm f}+I_{\rm p}=I$, where I is the total moment of inertia of the star. Due to magnetic couplings, the proton component essentially rotates at the observed pulsar angular velocity Ω.

We further assume that the pinned and non-pinned core superfluids are dynamically coupled to the proton fluid through mutual friction only. Although such a simple picture is a priori inadequate to describe the long-term post-glitch relaxation (for which additional processes such as vortex creep occur), our model can nevertheless be safely applied to the short spin-up stage. For simplicity, the mutual-friction coefficients associated with the pinned and non-pinned core superfluids, respectively, denoted by $\mathcal{B}_{\rm pin}$ and $\mathcal{B}_{\rm f}$, are supposed to be uniform and time independent. In other words, each vortex in the pinned region remains anchored to the same number $N_{\rm p}$ of fluxoids during the glitch rise. Mutual friction between the proton fluid and the core superfluid X is accounted for through the torque $\Gamma_X^i=\int_X\varepsilon^{ijk}x_j f_{Xk}\,{\rm d}^3V$, where $x^i=r\,\delta^i_r$ in spherical coordinates, f_X^k is the relevant mutual-friction force (5) and the integral is taken over the region X under consideration. Neglecting entrainment effects between the fluids, and assuming circular motion, the z-component of the torque simply reads $\Gamma_X^z=2\,\mathcal{B}_X\,I_{\rm n}^X\,\Omega_{\rm n}^X\left(\Omega_{\rm p}-\Omega_{\rm n}^X\right)$. The dynamics of the glitch rise is thus governed by the following equations:

$$\dot\Omega_{\rm p}=-\frac{I_{\rm n}^{\rm f}}{I_{\rm p}}\,\dot\Omega_{\rm n}^{\rm f}-\frac{I_{\rm n}^{\rm pin}}{I_{\rm p}}\,\dot\Omega_{\rm n}^{\rm pin}+\frac{\Gamma_{\rm ext}}{I_{\rm p}}\,, \tag{9}$$

$$\dot\Omega_{\rm n}^{\rm f}=2\,\mathcal{B}_{\rm f}\,\Omega_{\rm n}^{\rm f}\left(\Omega_{\rm p}-\Omega_{\rm n}^{\rm f}\right), \tag{10}$$

$$\dot\Omega_{\rm n}^{\rm pin}=2\,\mathcal{B}_{\rm pin}\,\Omega_{\rm n}^{\rm pin}\left(\Omega_{\rm p}-\Omega_{\rm n}^{\rm pin}\right), \tag{11}$$

where $\Gamma_{\rm ext}=I\dot\Omega_\infty$ stands for the external torque responsible for the slow braking of the pulsar on long time-scales with spin-down rate $\dot\Omega_\infty$.

3.2 Initial conditions and physical ingredients

In view of the lack of knowledge on the pre-glitch evolution, we simply assume that the proton component and the non-pinned core neutron superfluid at the beginning of the glitch ($t=0$) are rotating with a lag corresponding to the asymptotic post-glitch steady-state lag:[4] $\Omega_{\rm n}^{\rm f}(0)=\Omega_0+|\dot\Omega_\infty|/\left(2\,\mathcal{B}_{\rm f}\,\Omega_0\right)$ where $\Omega_0=\Omega_{\rm p}(0)$ (see e.g. Pizzochero, Montoli & Antonelli 2019). On the other hand, the initial rotation rate of the pinned core neutron superfluid is supposed to be given by $\Omega_{\rm n}^{\rm pin}(0)=\Omega_0+|\dot\Omega_\infty|/\left(2\,\mathcal{B}_{\rm pin}\,\Omega_0\right)+\delta\Omega_0$, where $\delta\Omega_0$ denotes a small deviation to the post-glitch steady-state lag.

To solve equations (9)−(11), the pulsar rotation rate Ω_0, the long-term spin-down rate $\dot\Omega_\infty$, the initial lag $\delta\Omega_0$, the mutual-friction coefficients $\mathcal{B}_{\rm f}$ and $\mathcal{B}_{\rm pin}$, and the ratios $I_{\rm n}^{\rm f}/I$ and $I_{\rm n}^{\rm pin}/I$ need to be specified. In what follows, Ω_0 and $\dot\Omega_\infty$ are directly taken from pulsar timing. The coefficient $\mathcal{B}_{\rm f}$ in the non-pinned region is given by $\mathcal{B}_0$, and the corresponding drag-to-lift ratio by equation (8). In the pinned region, the coefficient $\mathcal{B}_{\rm pin}$ is given by equation (6), with the prescription (7) and suitable parameters. Typical values for the underlying parameters are: $\varepsilon_{\rm p}^{\rm pin}\simeq 0.05-0.2$, $\varepsilon_{\rm p}^{\rm f}\simeq 0.1-0.5$ (see e.g. Chamel & Haensel 2006; Sourie, Oertel & Novak 2016), $x_{\rm p}^{\rm pin}\simeq 0.05-0.1$, $x_{\rm p}^{\rm f}\simeq 0.05-0.4$, $\rho_{\rm pin}\simeq(0.5-2)\rho_0$, and $\rho_{\rm f}\simeq(2-6)\rho_0$, $\rho_0\simeq 2.7\times10^{14}$ g cm^{-3} being the nuclear saturation density (see e.g. Pearson et al. 2018). The ratios $I_{\rm n}^{\rm pin}/I$ and $I_{\rm n}^{\rm f}/I$ are computed using the relations $I_{\rm n}^X/I^X=1-x_{\rm p}^X$ (assuming uniform densities in each region), where I^X is the total moment of inertia of region X, and $I^{\rm f}=I-I^{\rm cr}-I^{\rm pin}$, $I^{\rm cr}$ denoting the crustal moment of inertia of the star. Typical values are: $I^{\rm cr}/I\simeq 0.01-0.05$ (Delsate et al. 2016) and $I^{\rm pin}/I\sim 0.05$ (Gügercinoğlu & Alpar 2014). Unlike the previous quantities, both the initial lag $\delta\Omega_0$ and number $N_{\rm p}$ of pinned fluxoids are essentially unknown. As shown in the next section, the large range of possible values for $N_{\rm p}$ could account for the very different spin-up behaviours in the Crab and Vela pulsars.

[4]These post-glitch steady-state lags are obtained by imposing $\dot\Omega_{\rm n}^{\rm f}=\dot\Omega_{\rm n}^{\rm pin}=\dot\Omega_\infty$ in equations (10) and (11).

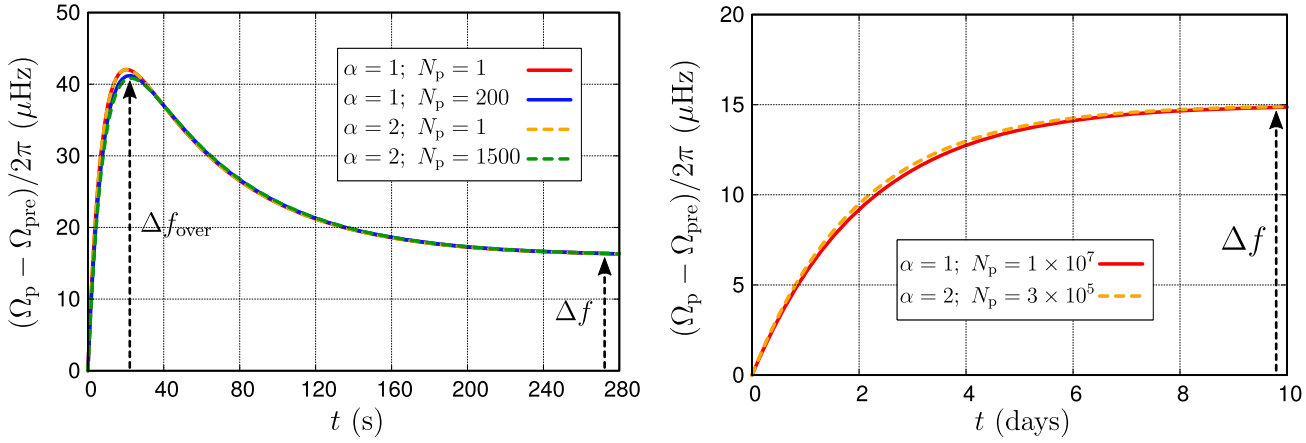

Figure 2. Left-hand panel: Evolution of the pulsar rotation frequency for parameters corresponding to the 2016 Vela glitch, plotted with respect to the rotation rate Ω_{pre} extrapolated from the pre-glitch evolution (i.e. in the absence of a glitch). Only the rise stage is considered. Solid (resp. dashed) lines correspond to results obtained for $\alpha = 1$ (resp. $\alpha = 2$). The evolution for $N_p = 1$ is independent of α, see equation (7). Right-hand panel: Similar to left-hand panel, but for input parameters corresponding to the 2017 Crab glitch. The smooth spin-up and the absence of overshoot can be explained by much larger values of N_p. See text for details.

3.3 Applications to the Crab and Vela pulsars

As discussed in the supplementary material (SM), the set of equations (9)–(11) can be solved analytically provided that the variations of the separate angular velocities are neglected with respect to those of the lags between the fluids appearing in the right-hand side of the equations[5] (see also Pizzochero et al. 2019). This analytical solution also allows for an unambiguous definition of the relevant time-scales governing the dynamics of the glitch rise. The adopted values for the different parameters are: $\varepsilon_p^{pin} = 0.05$, $x_p^{pin} = 0.07$, $\rho_{pin} = \rho_0$, $\varepsilon_p^{f} = 0.1$, $x_p^{f} = 0.2$, $\rho_f = 3\rho_0$, $I^{cr}/I = 0.03$, and $I^{pin}/I = 0.08$. This choice leads to $I_p/I \simeq 0.21$, $I_n^f/I \simeq 0.71$, and $I_n^{pin}/I \simeq 0.08$. The initial pulsar frequency $\Omega_0/2\pi$ is fixed to 11.19 Hz (resp. 29.64 Hz) for the Vela (resp. Crab) pulsar (Dodson et al. 2007; Shaw et al. 2018). Focusing on the deviation $\Delta\Omega_p(t) = \Omega_p(t) - \Omega_{pre}(t)$ induced by the glitch event in the evolution of the pulsar rotation rate, where $\Omega_{pre}(t) = \Omega_0 + \dot{\Omega}_\infty t$ is the rotation rate extrapolated from the pre-glitch evolution, the actual value of $\dot{\Omega}_\infty$ is unimportant.

Considering first the 2016 Vela glitch, the initial lag is fixed to $\delta\Omega_0 \simeq 1.351 \times 10^{-3}$ rad s^{-1} so that the final glitch amplitude is $\Delta f = 16$ μHz (see equation A.16 of the SM). The evolution of the pulsar rotation frequency $\Delta\Omega_p/(2\pi)$ is plotted in the left-hand panel of Fig. 2 for $\alpha = 1$, with $N_p = 1$ and 200, and $\alpha = 2$, with $N_p = 1$ and 1500. These values lead to an overshoot of magnitude $\Delta f_{over} \simeq 41$ μHz, a rise time-scale $\tau_r \simeq 8$ s and a decrease time-scale $\tau_d \simeq 57$ s, in close agreement with observations[6] (see Section 1). The reason for which different values of N_p (for a fixed α) lead to a similar spin-up evolution is discussed in sec. A2 of the SM. For intermediate values of N_p, the magnitude Δf_{over} of the overshoot would be larger and the rise time-scale τ_r would be shorter, τ_d remaining almost constant (see figs A2 and A3 of the SM). Conversely, for larger N_p, the rise time would increase and the magnitude of the overshoot would decrease until it disappears.

Regarding the 2017 Crab glitch, we set $\delta\Omega_0 = 1.267 \times 10^{-3}$ rad s^{-1}, so that $\Delta f = 15$ μHz. The corresponding evolution of the pulsar frequency $\Delta\Omega_p/(2\pi)$ is plotted in the right-hand panel of Fig. 2 for $\alpha = 1$ with $N_p = 1 \times 10^7$, and $\alpha = 2$ with $N_p = 3 \times 10^5$. Such large values of N_p lead to a much smoother increase in the pulsar rotation rate during the glitch rise (i.e. no overshoot), with a characteristic time-scale $\tau_r \simeq 2$ d, as observed (see Section 1).

As shown in the SM, observations of glitch overshoots set a lower bound on the moment of inertia of the non-pinned superfluid

$$\frac{I_n^f}{I} \geq 1 - \frac{\Delta f}{\Delta f_{over}}. \tag{12}$$

The most stringent constraint so far comes from the 2004 Vela glitch (Dodson et al. 2007), from which we deduce[7] $\Delta f \simeq 23$ μHz and $\Delta f_{over} \simeq 77$ μHz, leading to $I_n^f/I \gtrsim 0.70$. Moreover, there exists a critical value $N_p^{crit,\alpha}$ of N_p above which no overshoot can ever occur. The presence (absence) of an overshoot in Vela (Crab) glitches thus puts constraints on the maximum (minimum) number of pinned fluxoids.

4 DISCUSSIONS AND CONCLUSIONS

The standard scenario according to which the neutron superfluid in the core of an NS is strongly coupled to the crust on short time-scales and thus cannot take part to glitch events (Alpar et al. 1984) must be revised if vortices are pinned to N_p (potentially up to $\sim 10^{13}\, B_{12}\, P_{10}$) proton fluxoids. Using a three-component model, in which a pinned and a non-pinned core superfluids are dynamically coupled to the rest of the star through mutual friction, we have shown that the evolution of the pulsar rotation rate during the rise of a glitch can be very different depending on N_p. While a fast spin-up with an overshoot is expected for $1 \leq N_p \leq N_p^{crit,\alpha}$, higher values lead to a smooth rise (on a longer time-scale). The value of $N_p^{crit,\alpha}$ is determined by the mutual-friction coefficients. Vortex pinning can therefore account for the very different glitching behaviours observed in the Vela and Crab pulsars although the physical reason

[5]This assumption is well justified given the very small observed glitch amplitudes.

[6]The time-scales τ_r and τ_d given for Vela correspond respectively to the quantities τ_- and τ_+ introduced in the SM. For the Crab (see below), τ_r stands for τ_+, the lower time-scale $\tau_- \simeq 16.5$ s being completely negligible in this case.

[7]We interpret the shortest time-scale reported by Dodson et al. (2007) as τ_d. In their notations, we thus have $\Delta f = \Delta F_p$ and $\Delta f_{over} = \Delta F_p + \Delta F_1$.

for different N_p remains to be investigated. The difference may lie in the spatial arrangements of fluxoids, which in turn reflect different evolutions of the internal magnetic field in these stars. More information on the internal physics of NSs can be inferred from the details of the glitch rise. In particular, observations of an overshoot set a lower bound (12) on the moment of inertia of the non-pinned superfluid. Allowing N_p to evolve may explain other observed features such as a spin-down precursor or a delayed spin-up. Vortex pinning in the outer core of NSs may thus play a crucial role, not only for the post-glitch relaxation (Gügercinoğlu & Alpar 2014) but for all stages of the glitch dynamics.

As most previous studies, our analysis was carried out in the Newtonian framework. Although general relativistic effects may play a non-negligible role on the glitch rise (Sourie et al. 2017), their impact remains much smaller than that of vortex pinning. Still, our treatment remains very simplified. More realistic models require a better understanding of the local dynamics of individual vortices and fluxoids, as studied, e.g. by Drummond & Melatos (2018).

ACKNOWLEDGEMENTS

This work was supported by the Fonds De La Recherche Scientifique (Belgium) under grants no. 1.B.410.18F, CDR J.0115.18, and PDR T.004320.

REFERENCES

Alpar M. A., 2017, J. Astrophys. Astron., 38, 44
Alpar M. A., Langer S. A., Sauls J. A., 1984, ApJ, 282, 533
Andersson N., Sidery T., Comer G. L., 2006, MNRAS, 368, 162
Ashton G., Lasky P. D., Graber V., Palfreyman J., 2019, Nat. Astron., 3, 1143
Carter B., Chamel N., 2005, Int. J. Mod. Phys. D, 14, 717
Carter B., Langlois D., Prix R., 2002, Vortices in Unconventional Superconductors and Superfluids. Springer, Berlin, Heidelberg, p. 167
Chamel N., 2012, Phys. Rev. C, 85, 035801
Chamel N., 2017, J. Astrophys. Astron., 38, 43
Chamel N., Haensel P., 2006, Phys. Rev. C, 73, 045802
Delsate T., Chamel N., Gürlebeck N., Fantina A. F., Pearson J. M., Ducoin C., 2016, Phys. Rev. D, 94, 023008
Ding K. Y., Cheng K. S., Chau H. F., 1993, ApJ, 408, 167
Dodson R. G., McCulloch P. M., Lewis D. R., 2002, ApJ, 564, L85
Dodson R., Lewis D., McCulloch P., 2007, Ap&SS, 308, 585
Dommes V. A., Gusakov M. E., 2017, MNRAS, 467, L115
Drummond L. V., Melatos A., 2017, MNRAS, 472, 4851
Drummond L. V., Melatos A., 2018, MNRAS, 475, 910
Espinoza C. M., Lyne A. G., Stappers B. W., Kramer M., 2011, MNRAS, 414, 1679
Glampedakis K., Andersson N., Samuelsson L., 2011, MNRAS, 410, 805
Graber V., Cumming A., Andersson N., 2018, ApJ, 865, 23
Gügercinoğlu E., Alpar M. A., 2014, ApJ, 788, L11
Gusakov M. E., 2019, MNRAS, 485, 4936
Haber A., Schmitt A., 2017, Phys. Rev. D, 95, 116016
Hall H. E., Vinen W. F., 1956, Proc. R. Soc. A, 238, 215
Haskell B., Melatos A., 2015, Int. J. Mod. Phys. D, 24, 1530008
Haskell B., Pizzochero P. M., Seveso S., 2013, ApJ, 764, L25
Haskell B., Khomenko V., Antonelli M., Antonopoulou D., 2018, MNRAS, 481, L146
Jahan-Miri M., 2000, ApJ, 532, 514
Lyne A. G., Smith F. G., Pritchard R. S., 1992, Nature, 359, 706
Manchester R. N., 2017, Pulsar Glitches, Proc. IAU, Vol. 13. Cambridge University Press, p. 197
Mendell G., 1991, ApJ, 380, 515
Milner W. R. et al., 2019, Phys. Rev. Lett., 123, 173201
Palfreyman J., Dickey J. M., Hotan A., Ellingsen S., van Straten W., 2018, Nature, 556, 219
Pearson J. M., Chamel N., Potekhin A. Y., Fantina A. F., Ducoin C., Dutta A. K., Goriely S., 2018, MNRAS, 481, 2994
Pizzochero P., Montoli A., Antonelli M., 2019, preprint (arXiv:1910.00066)
Ruderman M., Zhu T., Chen K., 1998, ApJ, 492, 267
Sedrakian A. D., Sedrakian D. M., 1995, ApJ, 447, 305
Shaw B., Lyne A. G., Stappers B. W., et al., 2018, MNRAS, 478, 3832
Sourie A., Chamel N., 2020, MNRAS, in press, doi:10.1093/mnras/staa253
Sourie A., Oertel M., Novak J., 2016, Phys. Rev. D, 93, 083004
Sourie A., Chamel N., Novak J., Oertel M., 2017, MNRAS, 464, 4641
Srinivasan G., Bhattacharya D., Muslimov A. G., Tsygan A. J., 1990, Curr. Sci., 59, 31
Wong T., Backer D. C., Lyne A. G., 2001, ApJ, 548, 447

SUPPORTING INFORMATION

Supplementary data are available at *MNRASL* online.

Figure S1. Characteristic time-scales τ_+ and τ_- (A10) as functions of N_p for $\alpha = 1$ (solid lines) and $\alpha = 2$ (dashed lines).
Figure S2. Amplitude Δf_{over} of the overshoot as a function of N_p for $\alpha = 1$ (red solid line) and $\alpha = 2$ (orange dashed line).
Figure S3. Evolution of the pulsar frequency $\Delta\Omega_p/(2\pi)$, equation (A6), during the glitch rise for different values of N_p using $\alpha = 1$.

Please note: Oxford University Press is not responsible for the content or functionality of any supporting materials supplied by the authors. Any queries (other than missing material) should be directed to the corresponding author for the article.

This paper has been typeset from a TEX/LATEX file prepared by the author.